The Astrophysical Journal, 681:73–83, 2008 July 1

COEVOLUTION OF SUPERMASSIVE BLACK HOLES AND CIRCUMNUCLEAR DISKS

Nozomu Kawakatu and Keiichi Wada
National Astronomical Observatory of Japan, 2-21-1 Osawa, Mitaka, Tokyo 181-8588, Japan; kawakatu@th.nao.ac.jp
Received 2007 October 8; accepted 2008 March 14

ABSTRACT

We propose a new evolutionary model of a supermassive black hole (SMBH) and a circumnuclear disk (CND), taking into account the mass supply from a host galaxy and the physical states of the CND. In the model, two distinct accretion modes depending on the gravitational stability of the CND play a key role in accreting gas to a SMBH. (*i*) If the CND is gravitationally unstable, energy feedback from supernovae supports a geometrically thick, turbulent gas disk. The accretion in this mode is dominated by turbulent viscosity, and it is significantly larger than that in mode (*ii*), i.e., the CND is supported by gas pressure. Once the gas supply from the host is stopped, the high-accretion phase ($\sim$0.01–0.1 $M_\odot$ yr^{-1}) changes to the low one (mode [*ii*], $\sim 10^{-4}\,M_\odot$ yr^{-1}), but there is a delay of $\sim 10^8$ yr. Through this evolution, the gas-rich CND turns into the gas-poor stellar disk. We found that not all the gas supplied from the host galaxy to the central 100 pc region accretes onto the SMBH even in the high-accretion phase (mode [*i*]), because part of the gas is used to form stars. Outflow from the circumnuclear region also suppresses the growth of the SMBH. As a result, the final SMBH mass ($M_{\rm BH,final}$) is not proportional to the total gas mass supplied from the host galaxy ($M_{\rm sup}$); $M_{\rm BH,final}/M_{\rm sup}$ decreases with $M_{\rm sup}$. This would indicate that it is difficult to form a SMBH with $\sim 10^9\,M_\odot$ observed for high-z quasi-stellar objects. The evolution of the SMBH and CND would be related to the evolutionary tracks of different types of AGNs. We find that the AGN luminosity tightly correlates with the luminosity of the nuclear starburst only in the high-accretion phase (mode [*ii*]). This implies that the AGN-starburst connection depends on the evolution of the AGN activity.

Subject headings: black hole physics — galaxies: active — galaxies: nuclei — galaxies: starburst — ISM: structure

Online material: color figures

1. INTRODUCTION

The energy emitted by active galactic nuclei (AGNs) is commonly ascribed to accretion onto a supermassive black hole (SMBH). The recent discovery of powerful quasi-stellar objects (QSOs) at $z > 6$ (Fan et al. 2001) implies that the formation of SMBHs is completed in less than 1 Gyr. In addition, high-resolution observations of galactic centers indicate the presence of a SMBH whose mass correlates with the mass of the spheroidal stellar components of the galaxies, i.e., $M_{\rm BH}/M_{\rm sph} \approx 10^{-3}$ in the nearby universe (e.g., Kormendy & Richstone 1995; Marconi & Hunt 2003). These indicate that the formation and evolution of a SMBH and a spheroidal stellar component are closely related, despite 9 orders of magnitude difference in their size scale.

Various models have been proposed to explain the coevolution of AGNs and spheroids, or the physical link between the SMBH growth and the starburst in spheroids (e.g., Silk & Rees 1998; Adams et al. 2001; King 2003). However, little has been elucidated concerning the physics of angular momentum transfer in a spheroidal system (a bulge), which is inevitable for the formation of SMBHs, taking into account the tight connection between SMBHs and spheroids. Umemura (2001) proposed that the $M_{\rm BH}$-$M_{\rm sph}$ relation can be explained by the mass accretion onto the galactic center from a galactic scale ($\sim$1 kpc) via the radiation drag (see also Kawakatu & Umemura 2002). During the hierarchical formation of a galactic bulge, the mass accretion due to the tidal torque driven by the major and minor merger of galaxies would also be an important process for SMBH formations (e.g., Toomre & Toomre 1972; Mihos & Hernquist 1994; Mihos & Hernquist 1996; Saitoh & Wada 2004). However, previous studies of the coevolution model simply postulated that the mass accretion onto the BH horizon, $\dot{M}_{\rm BH}$, is regulated by the Eddington rate, $\dot{M}_{\rm Edd}$ (e.g., Umemura 2001; Kawakatu et al. 2003; Granato et al. 2004), or equals the mass supply rate from the host galaxy, $\dot{M}_{\rm sup}$ (e.g., Di Matteo et al. 2003; Kawata & Gibson 2005; Di Matteo et al. 2005; Okamoto et al. 2008).

The gas accumulated by galaxy mergers and radiation drags does not accrete onto a SMBH directly, since the angular momentum of the gaseous matter cannot be thoroughly removed. Thus, some residual angular momentum would terminate the radial infall, so the accreted gas forms a reservoir, i.e., a *circumnuclear disk*, in the central $\sim$100 pc around a SMBH (Fig. 1). In such a circumnuclear disk, the active star formation has been observed as the nuclear starburst ($<$100 pc) in nearby Seyfert galaxies (e.g., Imanishi & Wada 2004; Davies et al. 2007; Watabe et al. 2008). The nuclear starburst must affect the SMBH growth, because radiation and/or supernova (SN) feedback due to starbursts can trigger the mass accretion onto a SMBH (e.g., Umemura et al. 1997; Wada & Norman 2002, hereafter WN02). In order to understand the SMBH growth in terms of the evolutionary sequence of host galaxies, it is crucial to link mass accretion processes from a galactic scale with those from an accretion disk in the vicinity of a central BH, via the circumnuclear disk.

To this aim, it is necessary to construct a model of the circumnuclear disk. Recently, Thompson et al. (2005, hereafter T05) built up the radiation pressure-supported starburst disk with AGN fueling, considering the mass supply from host galaxies. In their model, they postulate external torques (e.g., bars and spiral waves) in order to ensure that the gas can accrete to the galactic center before it turns into stars. We here propose another plausible model of a nuclear starburst disk supported by the turbulent pressure led by SN explosions. WN02 examined the structure of matter around AGNs associated with starburst by three-dimensional hydrodynamic simulations. They showed that the internal gas motion is not steady and the matter is inhomogeneous, but the global geometry is supported by internal turbulence caused by SN explosions.

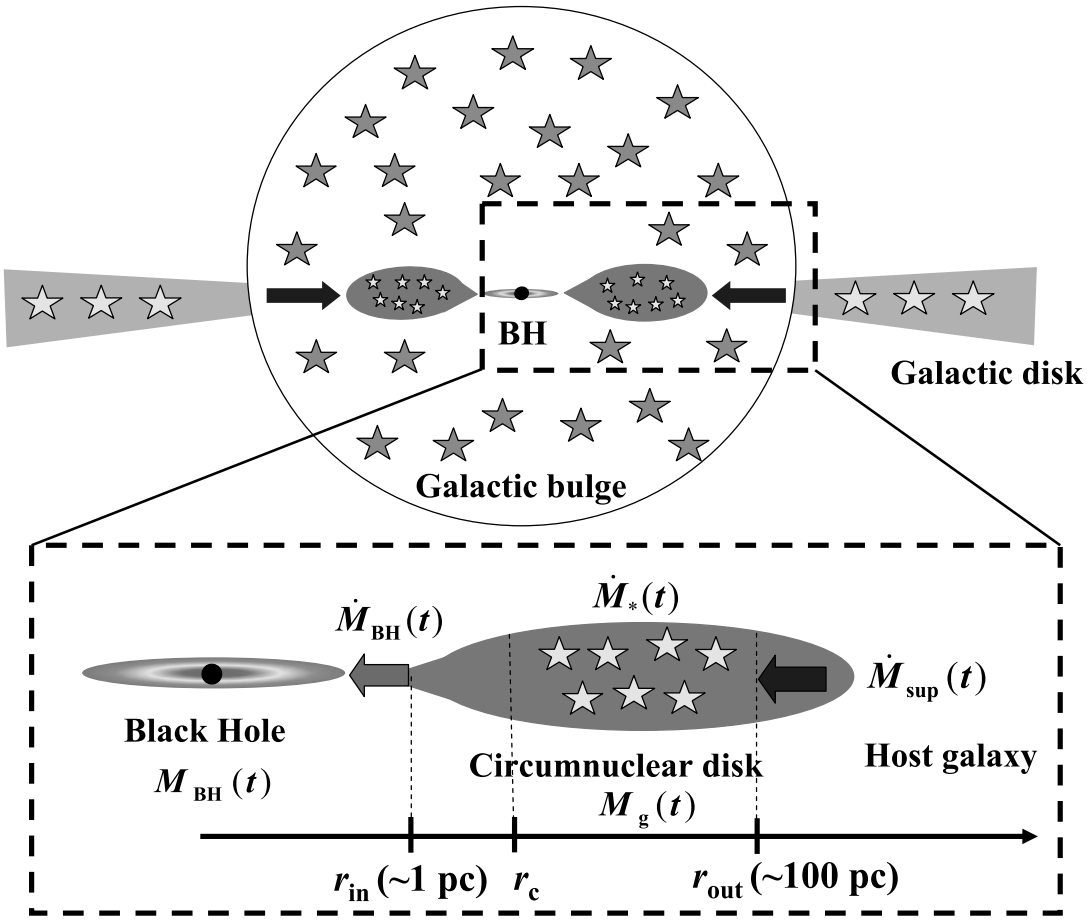

FIG. 1.—Schematic picture for a model of SMBH growth linked with the change of physical state in the circumnuclear disk supported by the turbulent pressure via SN explosions, where $r_{\rm in}$ and $r_{\rm out}$ are the inner radius and the outer radius, respectively. Star symbols represent the region where stars can form, i.e., $r > r_c$, where r_c is determined by the Toomre criterion (see § 2.2). Here, $M_{\rm BH}$, M_g, $\dot{M}_{\rm BH}$, $\dot{M}_*$, and $\dot{M}_{\rm sup}$ are the mass of the SMBH, the gas mass, the stellar mass, the BH growth rate, the star formation rate, and the mass supply rate from the host galaxy, respectively. [*See the electronic edition of the Journal for a color version of this figure.*]

They also observed the mass accretion ($\sim 0.1\ M_\odot\ {\rm yr}^{-1}$) to the central few pc region from the turbulent torus, and it is enhanced by the SN feedback. This means that the star formation and the gas accretion due to the turbulent viscosity can coexist in this inhomogeneous disk. Our model presented here relies on this picture, in which angular momentum is transferred by a turbulent viscosity. In our model, the mass accretion process, star formation, and the structure of the inhomogeneous circumnuclear disk are naturally combined. We elucidate how a SMBH grows from a seed BH, taking into account the mutual connection between the mass supply from a host galaxy and the physical states of the circumnuclear disk accompanied by the star formation. T05, on the other hand, did not discuss a long-term evolution of the circumnuclear disk and the central SMBH.

This article is arranged as follows. In § 2 we describe a new physical model for the circumnuclear disk supported by the turbulent pressure via SN explosions, considering the AGN fueling (§§ 2.1, 2.2, and 2.3). In § 2.4 we summarize the assumptions and free parameters in our model. In § 3 we first show how the growth rate of a SMBH changes with time (§ 3.1). Then, we examine the evolution of SMBHs and the gas and stellar masses in the disk (§ 3.2). Next, we examine the relation between the final mass of SMBHs and the total accreted gas mass from host galaxies (§ 3.3). In § 3.4 we elucidate the time evolution of AGN luminosity and the nuclear starburst luminosity. By comparing with observations, we predict the physical states of the circumnuclear disk for different types of AGNs. Finally, we show the AGN-starburst luminosity relation, and then we discuss the origin of the AGN–nuclear starburst connection (§ 3.5). In § 4 we discuss the effect of the AGN outflow and the radiation pressure caused by the young stars in disk. Moreover, we comment on the origin of a bias in AGN formation. Section 5 is devoted to our conclusions.

2. MODELS

We presuppose that the dusty gas is supplied around a central SMBH at a rate of $\dot{M}_{\rm sup}$ from a host galaxy whose surface density, $\Sigma_{\rm host}$, including the gas and stellar components, is constant in time. The accumulated gas forms a turbulent pressure-supported circumnuclear disk around a central SMBH with $M_{\rm BH}$ as schematically described in Figure 1. In this paper we focus on the average properties of the disk, although we take into account the physics in the inhomogeneous distribution of gas in the disk as we mention below. This treatment is valid because the global structure is dynamically stable even in the inhomogeneous distribution of gas in the disk on a local scale (see WN02).

2.1. *Turbulent Pressure-supported Circumnuclear Disk*

We describe the physical settings of the circumnuclear disk supported by the turbulent pressure via the SN explosions. From the radial centrifugal balance, the angular velocity $\Omega(r)$ is given by

$$\Omega(r)^2 = \frac{GM_{\rm BH}}{r^3} + \frac{\pi G}{r}[\Sigma_{\rm disk}(r) + \Sigma_{\rm host}], \qquad (1)$$

where $M_{\rm BH}$ is the mass of the BH and $\Sigma_{\rm disk}(r)$ is the surface density of baryonic components (the gaseous matter and stars).

Concerning the vertical structure of the circumnuclear disk, we assume hydrodynamical equilibrium. The turbulent pressure ($P_{\rm tub} = \rho_g v_t^2$) associated with SN explosions is balanced to gravity, g, caused by

$$\rho_g(r)v_t^2(r) = \rho_g(r)gh(r), \tag{2}$$

where $v_t(r)$ and $h(r)$ are the turbulent velocity and the scale height of the disk, respectively. Here, the gravity g is obtained as $g \equiv GM_{\rm BH}h/r^3 + \pi G[\Sigma_{\rm disk}(r) + \Sigma_{\rm host}]$.

The geometrical thickness is determined by the balance between the turbulent energy dissipation and the energy input from SN explosions. Thus, the energy balance in unit time and volume can be obtained as

$$\frac{\rho_g(r)v_t^2(r)}{t_{\rm dis}(r)} = \frac{\rho_g(r)v_t^3(r)}{h(r)} = \eta S_*(r)E_{\rm SN}, \tag{3}$$

where the dissipation timescale of the turbulence, $t_{\rm dis}(r)$, is assumed to be a crossing time, $h(r)/v_t(r)$, $E_{\rm SN}$ is the total energy (10^{51} erg) injected by an SN, η is the heating efficiency per unit mass which denotes how much energy from SNe is converted to the kinetic energy of the matter, and the star formation rate per unit volume and time is $S_*(r) = C_*\rho_g(r)$. Here, C_* is the star formation efficiency and $\rho_g(r) = \Sigma_g(r)/2h(r) = f_g\Sigma_{\rm disk}(r)/2h(r)$, where Σ_g is the surface density of the gas component in the disk and f_g is a gas fraction. In the inhomogeneous distribution of gas in the disk, the star formation can be led by gravitational collapse of clumps with a higher density than the critical density. Recently, Wada & Norman (2007) showed that the star formation rate, C_*, is approximately proportional to the average density, ρ_g, especially for a high-density end, if the statistical structure of gas density is represented by a log-normal probability distribution.

By using equations (2) and (3), the turbulent velocity and the scale height for the region where the central BH dominates the gravitational potential are given by

$$v_t(r) = \left(\frac{GM_{\rm BH}}{r^3}\right)^{1/2} h_{\rm tub}(r), \tag{4}$$

$$h_{\rm tub}(r) = \left(\frac{r^3}{GM_{\rm BH}}\right)^{3/4} (C_*\eta E_{\rm SN})^{1/2}, \tag{5}$$

where $h_{\rm tub}$ denotes the scale height supported by the turbulent pressure due to the SN feedback. We should emphasize that the validity of these solutions (eqs. [4] and [5]) were confirmed by comparison with WN02.

2.2. *Two Regimes of Gas Accretion in Circumnuclear Disk*

We suppose a kinetic viscosity as a source of angular momentum transfer in the gas disk. Then, we adopt the formula of mass accretion rate in a viscous accretion disk (Pringle 1981) as

$$\dot{M}(r) = -\left[\frac{(\partial/\partial r)G(r,t)}{(d/dr)[r^2\Omega(r)]}\right] = 2\pi\nu\Sigma_g(r)\left|\frac{d\ln\Omega(r)}{d\ln r}\right|, \tag{6}$$

where the viscous torque generated by the turbulent motion, G, is defined as $G(r,t) = 2\pi\nu_t(r)\Sigma_g(r)r^3\,d\Omega/dr$. Since the viscous parameter is expressed by $\nu_t(r) = \alpha v_t(r)h(r)$, the mass accretion rate in general increases as the energy input from SN explosions becomes large; in other words, the star formation rate is high (see eqs.[4] and [5]). Thus, the mass accretion rate depends on the gravitational stability of the disk. With respect to the stability, we adopt Toomre's stability criterion, i.e., when the surface density of gas in the disk, Σ_g, is higher (lower) than the critical surface density, $\Sigma_{\rm crit}$, the disk is gravitationally unstable (stable). The critical surface density is obtained as

$$\Sigma_{\rm crit}(r) = \frac{\kappa(r)c_s}{\pi G}, \tag{7}$$

where $\kappa(r) \equiv 4\Omega(r)^2 + 2\Omega(r)r\,d\Omega(r)/dr$ is the epicyclic frequency and c_s is the sound velocity. The critical radius r_c is determined by the Toomre criterion, that is, $\Sigma_g(r_c) = \Sigma_{\rm crit}(r_c)$.

In this picture, it is natural that there are two modes of gas accretion rate as follows.

Mode (*i*).—If the circumnuclear disk is fully gravitationally unstable, in other words, the critical radius for the gravitational instability, r_c, is smaller than the inner radius of the disk, $r_{\rm in}$, then the disk is geometrically thick due to stellar energy feedback, and as a result, we have a large accretion rate. The value of α produced by randomly distributed SN explosions is not obvious. However, thanks to numerical simulations demonstrated by WN02, the average transfer of angular momentum can be described as $\nu_t(r) \approx v_t(r)h(r)$. Thus, we suppose $\alpha = O(1)$.

Mode (*ii*).—If the critical radius is located inside the disk ($r_c > r_{\rm in}$), the scale height of the inner region would be much smaller than mode (*i*), because the scale height is determined by the thermal pressure, $P_g(r) = \rho_g(r)gh_{\rm th}(r)$, where $P_g(r) = \rho_g(r)c_s^2$. In mode (*ii*), the magnetorotational instability could be a source of turbulence, but the turbulent velocity is comparable to or even smaller than the sound speed, i.e., $\alpha \approx 0.01$–0.5 and $v_t = c_s$ (e.g., Balbus & Hawley 1991; Machida et al. 2000; Machida & Matsumoto 2003). As a result, the accretion is less efficient than mode (*i*). Since the critical radius and the inner edge of the disk are functions of the BH mass and the surface density of the gas, and the gas mass depends on the star formation rate in the gas disk, the evolution of the whole system (a central BH plus a circumnuclear disk) should be time dependent.

2.3. *SMBH Growth and States of the Circumnuclear Disk*

Based on the picture described in §§ 2.1 and 2.2, we here examine the evolution of central BHs and circumnuclear disks, considering the mass supply from host galaxies (see Fig. 1). For this purpose, we evaluate the time evolution of SMBH growth and the star formation rate and gas mass in the disk by focusing on the time dependence of the characteristic radius in the disk, instead of solving the evolution of the radial structure of disk. Then, the surface density of the disk is assumed to be a power law with the cylindrical radius r as $\Sigma_{\rm disk}(r) = \Sigma_{\rm disk,0}(r/r_{\rm out})^{-\gamma}$, where $r_{\rm out}$ is the outer boundary of the disk, which is defined below. Hereafter, the physical quantities with subscript 0 are the value at $r_{\rm out}$.

In this model, the supplied gas from the host galaxy is eventually consumed to form the SMBH or stars (see § 4.1 for the effect of AGN outflow). Then, the BH mass and the gas mass in the disk are simply given by the mass conservation as follows. The time evolution of the gas mass in the disk, $M_g \equiv \int_{r_{\rm in}}^{r_{\rm out}} 2\pi r'\Sigma_g(r')dr'$, is given by

$$M_g(t) = \int_0^t \left[\dot{M}_{\rm sup}(t') - \dot{M}_*(t') - \dot{M}_{\rm BH}(t')\right]dt', \tag{8}$$

where $\dot{M}_{\rm sup}(t)$, $\dot{M}_*(t)$, and $\dot{M}_{\rm BH}(t)$ are the mass supply rate from hosts, the star formation rate, and the growth rate of the SMBH,

respectively. On the other hand, the time evolution of the SMBH mass $M_{\rm BH}(t)$ is obtained as

$$M_{\rm BH}(t) = M_{\rm BH,seed} + \int_0^t \dot{M}_{\rm BH}(t')dt', \quad (9)$$

where we assume the mass of seed BHs, $M_{\rm BH,seed} = 10^3\ M_\odot$, as end products of the first-generation stars (e.g., Heger et al. 2003). As for $\dot{M}_{\rm sup}$, we can assume any function for the mass supply rate, but here we simply take a step function as the first attempt as

$$\dot{M}_{\rm sup}(t) = \begin{cases} \text{const}, & t < t_{\rm sup}, \\ 0, & t \geq t_{\rm sup}, \end{cases} \quad (10)$$

where $t_{\rm sup}$ is a period of the mass supply from hosts.

The star formation rate in the disk can be defined as $\dot{M}_* \equiv 2\int_{r_{\rm min}}^{r_{\rm out}} S_*(r')h(r')2\pi r'\,dr'$, where $r_{\rm min}$ is the minimum radius at which stars can form. Here, $r_{\rm min} = r_{\rm in}$ for $r_c < r_{\rm in}$ and $r_{\rm min} = r_c$ for $r_c > r_{\rm in}$. Thus, $\dot{M}_*(t)$ can be expressed in terms of $M_g(t)$ as follows,

$$\dot{M}_*(t) = AC_*M_g(t), \quad (11)$$

where $A = 1$ for $r_c < r_{\rm in}$, while $A = 1 - (r_c/r_{\rm out})^{3-\gamma}$ for $r_c > r_{\rm in}$.

We define the growth rate of the SMBH, $\dot{M}_{\rm BH}$, as $\dot{M}_{\rm BH} \equiv \dot{M}(r_{\rm in})$, where $\dot{M}(r_{\rm in})$ is the mass accretion rate in the inner region of the circumnuclear disk. By using equation (6), the BH growth rate is calculated for $0 \leq \gamma < 2$ as follows,

$$\dot{M}_{\rm BH} = \begin{cases} f_b\eta E_{\rm SN}\left(\dfrac{GM_{\rm BH}}{r_{\rm out}}\right)^{-1}\dot{M}_*\left(\dfrac{r_{\rm in}}{r_{\rm out}}\right)^{3-\gamma}, & \text{mode } (i), \\ 3f_{\rm geo}\left(\dfrac{\alpha c_s^3}{G}\right)\left(\dfrac{M_g}{M_{\rm BH}}\right)\left(\dfrac{r_{\rm in}}{r_{\rm out}}\right)^{2-\gamma}, & \text{mode } (ii), \end{cases} \quad (12)$$

where $f_b \equiv 3(14-4\gamma)(8-4\gamma)/16$ and $f_{\rm geo} \equiv r_{\rm in}/h(r_{\rm in})$.[1]

2.4. *Assumptions and Free Parameters*

In this section we summarize the assumptions and free parameters as follows.

Surface density of hosts $\Sigma_{\rm host}$.—We fix the surface density of host galaxies with $\Sigma_{\rm host} = 10^4\ M_\odot\ {\rm pc}^{-2}$. This is the upper value of nearby starburst galaxies (e.g., Kennicutt 1998), but may be a typical value of high-z starburst galaxies (e.g., Tacconi et al. 2006).

Surface density of disk $\Sigma_{\rm disk}(r)$.—As for the power-law surface density profile of the disk, we should note that recent numerical simulations of AGN disks showed that the single power-law profile is maintained (e.g., Levine et al. 2008). Such a power-law profile would be supported, because the turbulence generated by the self-gravity and/or the SN feedback redistributes the angular momentum in the disk on a dynamical timescale. In this paper we change the power-law index γ from 0 to 2.

Gas temperature of disk T_g.—As for the gas temperature, we assume the isothermal gas has $T_g = 100$ K, that is, $c_s \simeq 1$ km s^{-1}. Recent numerical simulations showed that the circumnuclear disk around a SMBH would be dominated by the cold gas ($T_g \approx$ 50–100 K), since the dust cooling is effective (e.g., Wada & Tomisaka 2005; see also Levine et al. 2008). In addition, the gas temperature is almost constant for the range of gas density in circumnuclear disks (Fig. 5 in Wada & Tomisaka 2005). These indicate that an isothermal gas with $T_g = 100$ K is a reasonable assumption for discussing mass evolution of the circumnuclear disk.

Outer radius $r_{\rm out}$.—The size $r_{\rm out}$ is defined as the outer boundary inside which the potential of the BH plus circumnuclear disk system dominates that of the host galaxy. From the Toomre condition, the outer part of the disk ($r > r_{\rm out}$) is always gravitationally stable, and then no stars can form in the disk. Since our main aim is to reveal the physical connection between the AGN activity (the SMBH growth) and the starburst in the circumnuclear region, we concentrate on the inner parts of the circumnuclear disk ($r < r_{\rm out}$). Then, when $M_{\rm disk} > M_{\rm BH}$ the outer radius $r_{\rm out}$ is given by $GM_{\rm disk}/r_{\rm out} = GM_{\rm BH}/r_{\rm out} + \pi G\Sigma_{\rm host}r_{\rm out}$, where $M_{\rm disk} \equiv \int_{r_{\rm in}}^{r_{\rm out}} 2\pi r'\Sigma_{\rm disk}(r')dr'$, and $r_{\rm in}$ is the inner radius of the disk. From equation (2), $r_{\rm out}$ is $\approx (M_{\rm disk}/\pi\Sigma_{\rm host})^{1/2} \sim 60$ pc $M_{\rm disk,8}^{1/2}\Sigma_{\rm host,4}^{-1/2}$, where $M_{\rm disk,8}$ and $\Sigma_{\rm host,4}$ are the total baryonic mass of the circumnuclear disk normalized by $10^8\ M_\odot$ and the surface density of host galaxy normalized by $10^4\ M_\odot\ {\rm pc}^{-2}$, respectively. On the other hand, if $M_{\rm disk} < M_{\rm BH}$, $r_{\rm out}$ is obtained from $GM_{\rm BH}/r_{\rm out} = \pi G\Sigma_{\rm host}r_{\rm out}$. From this, we quantitatively evaluate $r_{\rm out}$ as $r_{\rm out} = (M_{\rm BH}/\pi\Sigma_{\rm host})^{1/2} \sim 60$ pc $M_{\rm BH,8}^{1/2}\Sigma_{\rm host,4}^{-1/2}$, where $M_{\rm BH,8}$ is the mass of the BH normalized by $10^8\ M_\odot$.

Inner radius $r_{\rm in}$.—We suppose that the inner radius of the disk, $r_{\rm in}$, is determined by the dust sublimation radius, which is strongly supported by observational results (e.g., Suganuma et al. 2006). Thus, the inner radius $r_{\rm in}$ is expressed as $r_{\rm in} = 3$ pc $L_{\rm AGN,46}^{1/2}T_{1500}^{-2.8}$, where $L_{\rm AGN,46}$ is the AGN luminosity in units of 10^{46} erg s^{-1} and T_{1500} is the silicate grain sublimation temperature in units of 1500 K (Laor & Draine 1993). Although $r_{\rm in}$ depends on the size and composition of the dust grains (e.g., Barvainis 1992; Sitko et al. 1993; Laor & Draine 1993; Kishimoto et al. 2007), our conclusions do not change so much. Provided that $L_{\rm AGN}$ is equal to the Eddington luminosity, $L_{\rm Edd} = 4\pi cGM_{\rm BH}m_p/\sigma_{\rm T}$, the inner radius can be rewritten as $r_{\rm in} = 3{\rm pc}M_{\rm BH,8}^{1/2}T_{1500}^{-2.8}$, where m_p is the proton mass and $\sigma_{\rm T}$ is the Thomson cross section. In this paper we adopt $r_{\rm in} = 3$ pc $M_{\rm BH,8}^{1/2}$.

In our model, we have three free parameters as follows: (1) the power-law index of surface density, γ, (2) the heating efficiency, η, and (3) the star formation efficiency, C_*. In the following sections we use the fiducial values of $\gamma = 1$ and $\eta = 10^{-3}\ M_\odot^{-1}$, which can be derived from comparing our analytical solution of scale height with numerical simulations done by WN02, and $C_* = 3\times10^{-8}\ {\rm yr}^{-1}$, which is the upper value of nearby starburst galaxies (Kennicutt 1998; Fig. 13 in Wada & Norman 2007). However, since γ, η, and C_* are free parameters in this work we discuss the effect of changing these values in § 3.2. For these fiducial free parameters, $\dot{M}_{\rm BH}$ (eq. [12]), can be evaluated quantitatively as follows,

$$\frac{\dot{M}_{\rm BH}(t)}{M_\odot\ {\rm yr}^{-1}} = \begin{cases} 0.3\eta_{-3}C_{*,-8}\Sigma_{\rm host,4}^{1/2}M_{g,8}(t)M_{\rm disk,8}(t)^{-1/2}, & \text{mode } (i), \\ 3\times10^{-3}\alpha_{0.5}c_{s,1}^3\Sigma_{\rm host,4}^{1/4}M_{g,8}(t)M_{\rm disk,8}(t)^{-1/2}M_{\rm BH,8}(t)^{-1/4}, & \text{mode } (ii), \end{cases} \quad (13)$$

where η_{-3} is the heating efficiency normalized by $10^{-3}\ M_\odot^{-1}$, $C_{*,-8}$ is the star formation efficiency normalized by $10^{-8}\ {\rm yr}^{-1}$,

[1] Let us consider the dependences of $r_{\rm in}$, $r_{\rm out}$, M_g, M_*, and $M_{\rm BH}$ on $\dot{M}_{\rm BH}$ (see eq. [12]). For smaller $r_{\rm out}$ or larger $r_{\rm in}$, $\Sigma_g(r_{\rm in})$ increases because of $\Sigma_g(r) \propto r^{-\gamma}$ ($0 \leq \gamma < 2$). The larger $r_{\rm in}$ (or smaller $r_{\rm out}$) leads to larger $\dot{M}_{\rm BH}$, because $\dot{M}_{\rm BH} \propto \Sigma_g(r_{\rm in})$ from eq. (6). The larger BH mass leads to a smaller scale height from eq. (5). Thus, $\dot{M}_{\rm BH}$ becomes smaller since $\dot{M}_{\rm BH} \propto h$. As $\dot{M}_*$ ($\propto M_g$) and M_g are larger, $\Sigma_g(r_{\rm in})$ is larger, and thus, $\dot{M}_{\rm BH}$ increases.

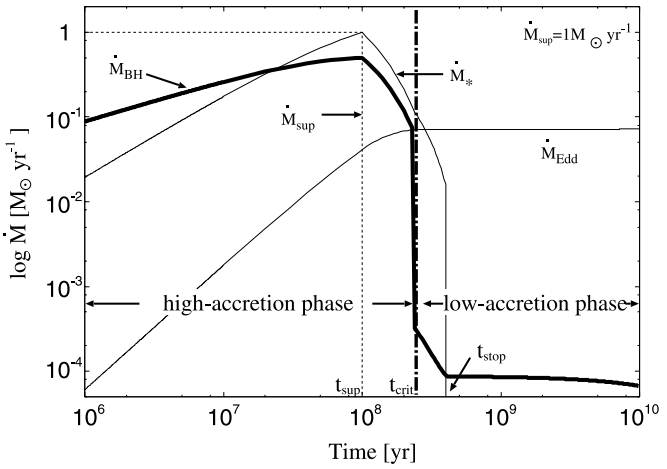

FIG. 2.—Time evolution of $\dot{M}_{\rm BH}(t)$, $\dot{M}_*(t)$, $\dot{M}_{\rm sup}(t)$, and $\dot{M}_{\rm Edd}(t)$ for $\dot{M}_{\rm sup} = 1\ M_\odot\ {\rm yr}^{-1}$ and $t_{\rm sup} = 10^8$ yr; $t_{\rm sup}$ is the period of mass supply from hosts, $t_{\rm crit}$ is the time when $r_c = r_{\rm in}$, and $t_{\rm stop}$ is the time when the massive disk is gravitationally stable, that is, $\Sigma_g < \Sigma_{\rm crit}$ for the entire massive disk. We call the phase $t < t_{\rm crit}$ the high-accretion phase, while we call the phase $t > t_{\rm crit}$ the low-accretion phase. The star formation efficiency C_* is 3×10^{-8} yr^{-1}.

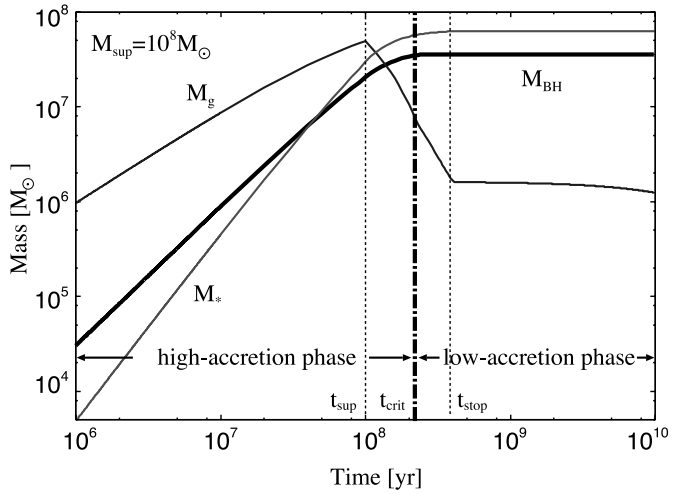

FIG. 3.—Time evolution of the mass of BH (*black solid line*), $M_{\rm BH}(t)$, the gas mass in the disk (*dark gray solid line*), $M_g(t)$, and the stellar mass in the disk (*light gray solid line*), $M_*(t)$. The total supplied mass from host galaxies $M_{\rm sup}$ is $10^8\ M_\odot$. The star formation efficiency C_* is 3×10^{-8} yr^{-1}. Note that $m_{\rm disk} \equiv M_g/M_{\rm BH}$ and $f_g \equiv M_g/(M_g + M_*)$. [*See the electronic edition of the Journal for a color version of this figure.*]

$M_{g,8}$ is the gas mass of the massive disk normalized by $10^8\ M_\odot$, $\alpha_{0.5}$ is the α-parameter normalized by 0.5, and $c_{s,1}$ is the sound velocity normalized by 1 km s^{-1}.

3. RESULTS

3.1. *The Growth Rate of SMBHs and Star Formation Rate*

Based on the physical model connecting the growth of SMBHs and the physical states of circumnuclear disks described in § 2, we examine how the growth rate of SMBHs is related to the star formation rate in the circumnuclear disk. Figure 2 shows the time evolution of $\dot{M}_{\rm BH}(t)$, $\dot{M}_*(t)$, and $\dot{M}_{\rm Edd}(t) \equiv L_{\rm Edd}(t)/c^2$ for $\dot{M}_{\rm sup} = 1\ M_\odot\ {\rm yr}^{-1}$ and $t_{\rm sup} = 10^8$ yr. The critical timescale, $t_{\rm crit}$, is the time when $r_c = r_{\rm in}$. Thus, the stars can form in the whole region of the disk before $t = t_{\rm crit}$. We define the former phase ($t < t_{\rm crit}$) as the high-accretion phase and the latter phase ($t > t_{\rm crit}$) as the low-accretion phase. As seen in Figure 2, we find that not all the gas supplied from a host galaxy reaches the SMBH, i.e., $\dot{M}_{\rm BH} = 0.1$–$0.3\ M_\odot\ {\rm yr}^{-1}$ for $\dot{M}_{\rm sup} = 1\ M_\odot\ {\rm yr}^{-1}$ even in the high-accretion phase ($r_c < r_{\rm in}$). This high-accretion phase drastically changes to the low-accretion phase with $\dot{M}_{\rm BH} \sim 10^{-4}\ M_\odot\ {\rm yr}^{-1}$. But, there is a delay of $\sim 10^8$ yr after the mass supply is stopped. The disk becomes gravitationally stable because the surface density of gas in the disk decreases due to the star formation. Thus, this timescale is basically determined by the star formation timescale, $t_* = C_*^{-1} \sim 3 \times 10^7$ yr. The drastic change of $\dot{M}_{\rm BH}$ depends on whether stars are formed in the inner region of the circumnuclear disk, because the ratio of $\dot{M}_{\rm BH}$ between the high- and low-accretion phases is given by

$$\frac{\dot{M}_{\rm BH}(r_c < r_{\rm in})}{\dot{M}_{\rm BH}(r_c > r_{\rm in})} = \frac{v_t h_{\rm tub}}{\alpha c_s h_{\rm th}} \sim 10^3,$$

where $v_t/(\alpha c_s) \approx 10^2 M_{\rm BH,8}^{1/8}$ and $h_{\rm tub}/h_{\rm th} \approx 10 M_{\rm BH,8}^{1/8}$.

It also has been found that SMBH growth dominates the star formation in the disk (i.e., $\dot{M}_{\rm BH} > \dot{M}_*$) in the early epoch, i.e., $t < t_* = C_*^{-1} \sim 3 \times 10^7$ yr. In this phase, a super-Eddington mass accretion rate ($\dot{M}_{\rm BH} \gg \dot{M}_{\rm Edd}$) is maintained for $\sim 10^8$ yr. Recent two-dimensional radiation hydrodynamic simulations have shown that such a super-Eddington mass accretion flow is possible (e.g., Ohsuga et al. 2005). After this phase, $\dot{M}_*$ is larger than $\dot{M}_{\rm BH}$ because of $\dot{M}_* \propto t$ and $\dot{M}_{\rm BH} \propto t^{1/2}$.[2] Then, the SMBH growth rate is much smaller than the Eddington mass accretion rate because of the gas pressure–supported geometrically thin disk. After $t = t_{\rm stop}$ the star formation terminates because the entire disk is gravitationally stable, where $t_{\rm stop}$ is the time when $\Sigma_g(r)$ is smaller than $\Sigma_{\rm crit}(r)$ throughout the entire circumnuclear disk.

3.2. *Evolution of Gas, SMBH, and Stellar Masses*

In this section we elucidate the physical difference between two phases for SMBH growth (high- and low-accretion phases). We plot the mass of the SMBH, $M_{\rm BH}(t)$, the gas mass in the disk, $M_g(t)$, and the stellar mass in the disk, $M_*(t) \equiv \int_0^t \dot{M}_*(t')dt'$ in Figure 3. The total supplied gas mass from the hosts, $M_{\rm sup} \equiv \dot{M}_{\rm sup} t_{\rm sup}$, is $10^8\ M_\odot$. In the high-accretion phase, plenty of gas accumulates around a SMBH, since $\dot{M}_{\rm sup}(t) > \dot{M}_{\rm BH}(t)$ (see Fig. 2). Thus, the mass ratio of gas in the circumnuclear disk and the SMBH, $m_{\rm disk} \equiv M_g/M_{\rm BH}$, is about 10 and the gas fraction to the total baryonic mass, $f_g \equiv M_g/(M_g + M_*)$, is close to ≈ 1. Recalling that the accretion is super-Eddington in the high-accretion phase, large $m_{\rm disk} > 1$ and $f_g \sim 1$ would be the conditions which super-Eddington mass accretion can keep. Since the scale height in the inner region is inflated by the energy input led by the SN explosions, the circumnuclear disk would be geometrically thick, which may correspond to the obscuring torus proposed by the AGN unified model (e.g., Antonucci 1993; Urry & Padovani 1995; WN02). On the other hand, in the low-accretion phase ($t > t_{\rm crit}$), stellar mass dominates the BH mass and gas mass, i.e., $f_g \approx 10^{-2}$ and $m_{\rm disk} \approx 0.03$. In this phase, the disk is gravitationally stable, so that the inner region of the disk should be geometrically thin.

Moreover, we find that the saturation of SMBH growth appears $\sim 10^8$ yr later after the mass supply is stopped. One should note that the final BH mass is about 1/3 of the total gas mass supplied

[2] During $t < t_{\rm sup}$, $\dot{M}_{\rm BH} \propto M_g^{1/2}$ because $M_{\rm disk}$ is nearly equal to M_g from eq. (12). On the other hand, $\dot{M}_* \propto M_g$ from eq. (11), considering $M_g \propto t$ until $t = t_{\rm sup}$ (see Fig. 3).

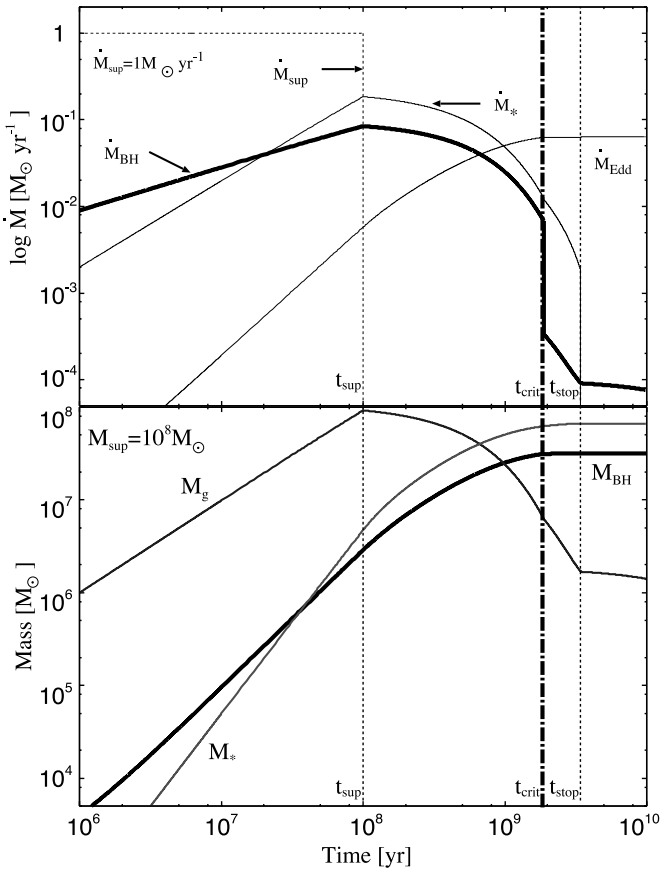

FIG. 4.—Same as Figs. 2 and 3, but the star formation efficiency C_* is 10 times smaller (i.e., $C_* = 3 \times 10^{-9}$ yr^{-1}). [*See the electronic edition of the Journal for a color version of this figure.*]

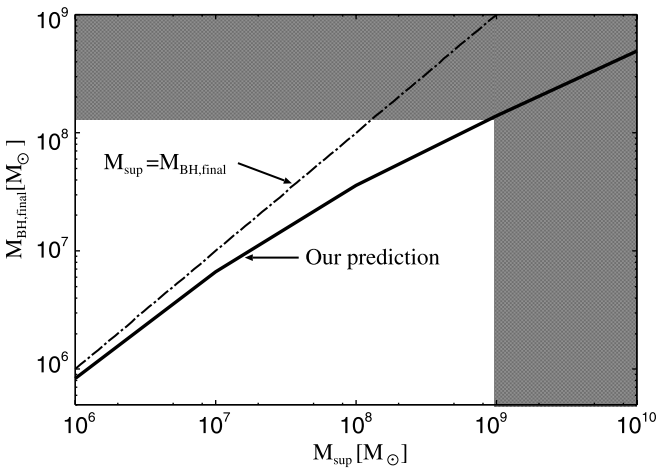

FIG. 5.—Final SMBH mass, $M_{\rm BH,final}$, against the different total accreted mass from host galaxies, $M_{\rm sup} \equiv \dot{M}_{\rm sup} t_{\rm sup}$, for $t_{\rm sup} = 10^8$ yr. The thick solid line shows our prediction. The dot-dashed line denotes $M_{\rm BH,final} = M_{\rm sup}$. We show the parameter space of $M_{\rm sup}$ and $M_{\rm BH,final}$, which are hard to achieve by any plausible mass supply process ($M_{\rm sup} > 10^9\ M_\odot$ and $M_{\rm BH,final} > 10^8\ M_\odot$), as the shaded region. Note that our prediction does not depend on C_* or $t_{\rm sup}$ (see §§ 3.2 and 3.3).

from hosts. The timescale of the SMBH growth, $t_{\rm growth}$, is determined by the viscous timescale, $t_{\rm vis}$, in the disk as follows,

$$\frac{t_{\rm vis}}{10^8\ {\rm yr}} \approx \frac{r_{\rm in}^2}{v_t h} = \frac{G M_{\rm BH,final}}{\eta E_{\rm SN} r_{\rm in}} C_*^{-1} \sim 5 \left(\frac{\eta}{10^{-3}\ M_\odot^{-1}}\right)^{-1} \left(\frac{M_{\rm BH,final}}{10^8\ M_\odot}\right)^{1/2} \left(\frac{t_*}{10^8\ {\rm yr}}\right), \quad (14)$$

where $M_{\rm BH,final}$ is the final SMBH mass. At given $\eta = 10^{-3}\ M_\odot^{-1}$ and $M_{\rm BH,final} = 3 \times 10^7\ M_\odot$ (see Fig. 3), the timescale of SMBH growth is comparable to that of star formation in the gas disk. From equation (14), it is found that the rapid BH growth (i.e., $t_{\rm growth} < 10^9$ yr) can be achieved if the star formation rate in the disk is quite high, e.g., $t_* \leq 10^8$ yr. Hence, it is essential to reveal what determines the star formation timescale (i.e., the star formation efficiency, C_*) in the circumnuclear disk. This will be left for our future works. We can understand the dependence of η and $M_{\rm BH,final}$ as follows. From equation (5), the larger BH mass leads to a smaller scale height, so that $t_{\rm growth}$ becomes larger as $M_{\rm BH,final}$ increases because of $\dot{M}_{\rm BH} \propto h$. Since $\dot{M}_{\rm BH} \propto \eta$ (see eq. [12]), $t_{\rm growth}$ is longer as η becomes larger.

Finally, we discuss the effect of three free parameters (γ, C_*, and η). As for γ, we examine $\dot{M}_{\rm BH}$ for $\gamma = 0.5$ and 1.5 by using the analytical solutions (see eq. [12]) and find that our results do not depend on the difference of γ significantly, that is, the difference in $\dot{M}_{\rm BH}$ between $\gamma = 1$ and 0.5 (or 1.5) is less than a factor of 2, although $\dot{M}_{\rm BH}$ is larger for larger γ. For C_*, both the star formation rate and BH growth rate in the high-accretion phase are 10 times smaller from equations (11) and (12), if we adopt 10 times smaller C_*, i.e., $C_* = 3 \times 10^{-9}$ yr^{-1}. Thus, after $t_{\rm sup}$ the gas mass in the disk decreases slower (see eq. [8]), and then $t_{\rm crit}$ and $t_{\rm stop}$ become roughly 10 times longer. However, the final BH mass ($M_{\rm BH,final} \approx \dot{M}_{\rm BH} t_{\rm growth}$) does not change significantly because of $\dot{M}_{\rm BH} \propto C_*$ and $t_{\rm growth} \propto C_*^{-1}$. This is confirmed by Figure 4, which is the same as Figures 2 and 3, but the star formation efficiency is 10 times smaller (i.e., $C_* = 3 \times 10^{-9}$ yr^{-1}). Concerning η, if η is 10 times smaller than the value we adopted, i.e., $10^{-4}\ M_\odot^{-1}$, the final BH mass is 10 times smaller because of $\dot{M}_{\rm BH} \propto \eta$ in the high-accretion phase (see eq. [12]).

3.3. $M_{\rm BH,final}$-*to*-$M_{\rm sup}$ *Relation*

As mentioned in § 3.2, the final mass of the SMBH, $M_{\rm BH,final}$, is not equal to $M_{\rm sup}$, i.e., $M_{\rm BH,final} \approx 0.3 M_{\rm sup}$. In this section we examine the relation between $M_{\rm BH,final}$ and $M_{\rm sup}$. Figure 5 shows the final BH mass as a function of the total accreted mass from host galaxies with $M_{\rm sup} = 10^6$–$10^{10}\ M_\odot$. We here assume $t_{\rm sup} = 10^8$ yr. Since the solid line is our prediction and the dot-dashed line denotes $M_{\rm BH,final} = M_{\rm sup}$, it is found that $M_{\rm BH,final}/M_{\rm sup}$ gets smaller as $M_{\rm sup}$ becomes larger, i.e., $M_{\rm BH,final}/M_{\rm sup} = 0.8, 0.6, 0.3, 0.1$, and 0.05 for $M_{\rm sup} = 10^6$, 10^7, 10^8, 10^9, and $10^{10}\ M_\odot$, respectively. In other words, the final mass of SMBHs, $M_{\rm BH,final}$, is not proportional to $M_{\rm sup}$, and the growth of a SMBH is more inefficient for larger $M_{\rm sup}$. As mentioned in §§ 3.1 and 3.2, the star formation in the disk dominates the growth of the SMBH as $M_{\rm sup}$ increases. As a result, all the gas accreted from hosts cannot accrete onto a central SMBH, but turns into stars in the late phase of mass supply. The above trend does not change for $t_{\rm sup} = 10^7$–10^9 yr and also for changing the star formation efficiency, C_*.

The averaged mass supply rate, $\dot{M}_{\rm sup}$, is expected to be typically $\approx$0.1–1 $M_\odot$ yr^{-1}, driven by galaxy mergers (e.g., Mihos & Hernquist 1996; Saitoh & Wada 2004) or by the radiation drag associated with the starbursts in hosts (e.g., Umemura 2001; Kawakatu & Umemura 2002). Thus, it may be hard to accrete the gas mass more than $\approx 10^9\ M_\odot$ from the host galaxy for 10^8–10^9 yr. Even if the gas supply with 1 $M_\odot$ yr^{-1} lasts for 10^9 yr, a SMBH does not evolve more than $10^8\ M_\odot$. This would imply that it is difficult for only the gas accretion process due to the turbulent viscosity driven by SN explosions to form a SMBH $>10^9\ M_\odot$ observed in the luminous high-z QSOs (e.g., McLure et al. 2006).

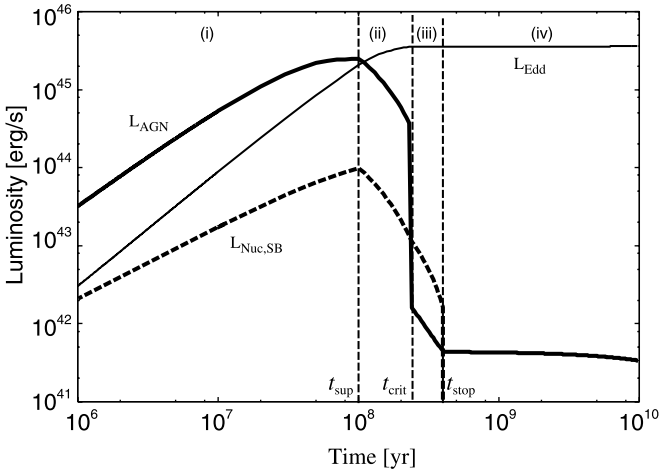

FIG. 6.—Time evolution of the AGN luminosity, $L_{AGN}(t)$, that of the nuclear starburst luminosity, $L_{nuc,SB}(t)$, and that of the Eddington luminosity, $L_{Edd}(t)$. We can divide this into the four phases as follows: (*i*) $t < t_{sup}$, (*ii*) $t_{sup} < t < t_{crit}$, (*iii*) $t_{crit} < t < t_{stop}$, and (*iv*) $t > t_{stop}$. These phases (*i*), (*ii*), (*iii*), and (*iv*) correspond to the super-Eddington luminosity phase, the sub-Eddington luminosity phase, the starburst luminosity–dominated phases, and the post-AGN/starburst phase, respectively.

3.4. *Evolution of AGN Luminosity and Nuclear Starburst Luminosity*

We examine the evolution of the AGN luminosity and the nuclear starburst luminosity (the luminosity originating in star formation in the circumnuclear disk), in order to understand which objects correspond to these two phases observationally. In this paper we define these luminosities as follows. The AGN luminosity (the accretion disk luminosity) can be obtained as a function of $\dot{m}_{BH} \equiv \dot{M}_{BH}/\dot{M}_{Edd}$ (Watarai et al. 2000), by assuming two types of accretion disks, namely, the slim disk (Abramowicz et al. 1988) and the standard disk (Shakura & Sunyaev 1973),

$$L_{AGN}(t) = \begin{cases} 2\left[1 + \ln\dfrac{\dot{m}_{BH}(t)}{20}\right] L_{Edd}(t), & \dot{m}_{BH}(t) \geq 20, \\ \left[\dfrac{\dot{m}_{BH}(t)}{10}\right] L_{Edd}(t), & \dot{m}_{BH}(t) < 20. \end{cases} \quad (15)$$

The nuclear starburst luminosity $L_{nuc,SB}(t)$ can be given by

$$L_{nuc,SB}(t) = 0.14\epsilon\dot{M}_*(t)c^2, \quad (16)$$

where $\epsilon = 0.007$ which is the energy conversion efficiency of nuclear fusion from hydrogen to helium.

Figure 6 shows the evolution of AGN luminosity $L_{AGN}(t)$ and nuclear starburst luminosity $L_{nuc,SB}(t)$ for $\dot{M}_{sup} = 1\ M_\odot\ \mathrm{yr}^{-1}$ and $t_{sup} = 10^8$ yr. The mass accretion in units of the Eddington mass accretion rate $\dot{m}_{BH}$ is larger than 20 until $t = t_{sup}$ (see Fig. 2). Then, $L_{AGN}(t)$ depends on the evolution of $L_{Edd}(t) \propto M_{BH}(t)$ from equation (15), and thus, $L_{AGN}(t)$ increases with time. During this phase ($t < t_{sup}$), the nuclear starburst luminosity, $L_{nuc,SB}(t) \propto \dot{M}_*(t) \propto M_g(t)$, also increases with time because $M_g(t)$ increases (see Fig. 3). After $t = t_{sup}$, both $L_{AGN}(t)$ and $L_{nuc,SB}(t)$ decrease, since M_g starts to decrease monotonically (see Fig. 3). The AGN luminosity decreases drastically after $t = t_{crit}$, reflecting the phase change of accretion (see Fig. 2). After $t = t_{stop}$, $L_{nuc,SB}$ becomes zero because the circumnuclear disk is gravitationally stable as mentioned in § 3.1. In summary, there are four phases in $L_{AGN}(t)$ and $L_{nuc,SB}(t)$: (*i*) the super-Eddington luminosity phase $L_{AGN} > L_{Edd}$ ($t < t_{sup}$); (*ii*) the sub-Eddington luminosity phases $L_{AGN} = (0.1\text{–}1)L_{Edd}$ ($t_{sup} < t < t_{crit}$); (*iii*) the starburst luminosity–dominated phase $L_{AGN} < L_{nuc,SB} \ll L_{Edd}$ ($t_{crit} < t < t_{stop}$); and (*iv*) the post-AGN/starburst phase $L_{AGN} \ll L_{Edd}$ and $L_{nuc,SB} = 0$ ($t > t_{stop}$).

Phase (*i*) might be a good model for narrow-line type I Seyfert galaxies (NLS1s), because NLS1s are super-Eddington AGNs (e.g., Mathur et al. 2000; Kawaguchi 2003). On the other hand, if the mass supply is extremely high (e.g., $\dot{M}_{sup} = 10\ M_\odot\ \mathrm{yr}^{-1}$) and consequently the circumnuclear region is covered by dense gas, then this phase might be observed as ultraluminous infrared galaxies (ULIRGs). Note that some kinds of ULIRGs show properties similar to NLS1s (e.g., Teng et al. 2005; Hao et al. 2005; Kawakatu et al. 2007b). If this is the case, we predict that *a gas-rich massive torus* ($m_{disk} > 1$ and $f_g = 1$) exists at their center. Such a massive torus can be observed through carbon monoxide and hydrogen cyanide molecular emission using the Atacama Large Millimeter Array instrument (ALMA) for NLS1s and ULIRGs (e.g., Wada & Tomisaka 2005; Kawakatu et al. 2007a; Yamada et al. 2007). Judging from the luminosity ratio ($L_{AGN}/L_{Edd} = 0.1\text{–}1$), in phase (*ii*) the AGNs are still bright, and thus, these might be broad-line type I Seyfert galaxies (BLS1s) or QSOs. In this phase, the relatively small m_{disk} and f_g are predicted, i.e., $m_{disk} = 0.2\text{–}1$ and $f_g \approx 0.1\text{–}0.5$. After phase (*ii*), the AGN luminosity becomes smaller by 3 orders of magnitude than its peak luminosity. Thus, phases (*iii*) and (*iv*) may correspond to the low-luminosity AGNs (LLAGNs) associated with and without the nuclear starburst, respectively. As seen in Figure 3, *a geometrically thin massive stellar disk*, i.e., $M_* > M_{BH}$ and $f_g \approx 10^{-2}$, is expected in this post-AGN phase. Thus, this indicates that the LLAGNs do not have obscuring tori envisaged in the AGN unified model, because no stars form near the inner radius of the circumnuclear disk. In other words, we predict the absence of obscuring tori in LLAGNs. This seems to be consistent with observations that most low-luminosity radio galaxies (FR I) show no evidence of dusty tori expected in normal AGNs (e.g., Chiaberge et al.1999). As an alternative explanation, Elitzur & Shlosman (2006) suggested that the torus disappears when the AGN luminosity decreases below $\sim 10^{42}$ erg s^{-1}, because the mass accretion in the accretion disk cannot maintain the required cloud outflow (see also Hönig & Beckert 2007). In order to understand the origin of the absence of dusty tori in LLAGNs, it is essential to explore the spatial distribution of young stars in them. In addition, since such a stellar disk is a remnant of a gas-rich massive torus in the early phase of SMBH growth, its discovery would strongly support the idea that LLAGNs are dead Seyfert galaxies or QSOs. Therefore, the observations of the physical states of a circumnuclear disk on $\leq$100 pc, e.g., m_{disk} and f_g, for different type of AGNs would be useful to understand AGN evolution.

Finally, we summarize a coevolution scenario of SMBHs and circumnuclear disks in Figure 7. According to our knowledge obtained in this paper, we might guess that the final state of AGNs depends on the mass supply rate $\dot{M}_{sup}$ and the duration of the mass supply t_{sup}. We will discuss this issue in detail in our upcoming paper.

3.5. *AGN Luminosity Versus Nuclear Starburst Luminosity Relation*

Based on our model, we present the correlation between AGN luminosity and nuclear starburst luminosity. In Figure 8 we plot $L_{nuc,SB}$ against L_{AGN} for the different $M_{BH,final}$ (or M_{sup}). The higher concentration of data points represents that the evolution is slow. We find that AGN luminosity positively correlates with nuclear starburst luminosity for bright AGNs (right branches of Fig. 8),

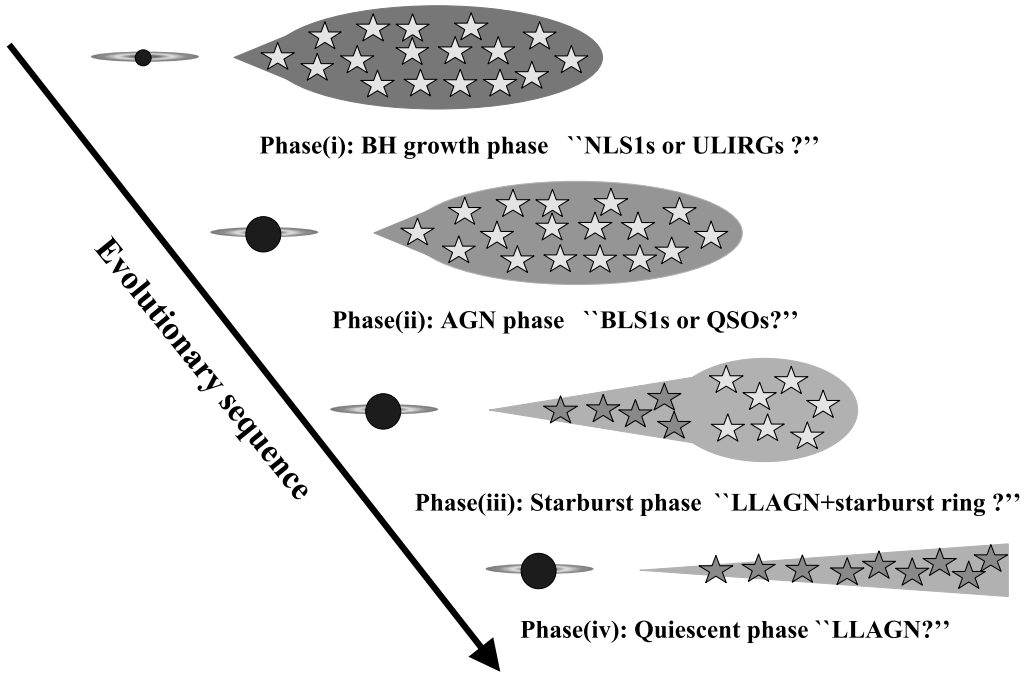

FIG. 7.—Schematic sketch for the coevolution of a SMBH and a circumnuclear disk. Star symbols (*light gray*) represent young stars. Star symbols (*dark gray*) denote old stars. The darkness of the gray color in the background shows the gas fraction (f_g), that is, the darker gray represents higher gas fraction. [*See the electronic edition of the Journal for a color version of this figure*.]

which corresponds to the high-accretion phase, that is, phases (*i*) and (*ii*) defined in § 3.4. This trend is consistent with the observational results for nearby Seyfert galaxies (Imanishi & Wada 2004; Watabe et al. 2008). Moreover, $L_{\rm nuc,SB}/L_{\rm AGN}$ becomes larger as $L_{\rm AGN}$ increases. This can be explained as follows: $L_{\rm nuc,SB}/L_{\rm AGN}$ ($\propto \dot{M}_*/\dot{M}_{\rm BH}$) is larger as M_g increases because of $\dot{M}_*/\dot{M}_{\rm BH} \propto M_g^{1/2}$ (see § 3.1). Considering $L_{\rm AGN} \propto \dot{M}_{\rm BH} \propto M_g^{1/2}$ during $t < t_{\rm sup}$, $L_{\rm nuc,SB}/L_{\rm AGN}$ increases with $L_{\rm AGN}$. We should mention that it is worth examining this trend with future observations.

On the other hand, the $L_{\rm AGN}$ versus $L_{\rm nuc,SB}$ relation in LLAGNs (left branches of Fig. 8) does not follow that in bright AGNs. In this phase, the range of AGN luminosity is independent of $L_{\rm nuc,SB}$, i.e., $L_{\rm AGN} = 10^{41}$–10^{42} erg s^{-1} for $L_{\rm nuc,SB} = 10^{40}$–10^{44} erg s^{-1}, because $\dot{M}_{\rm BH}$ is basically determined by the sound velocity in the disk. Since the nuclear starburst luminosity, $L_{\rm nuc,SB} \propto \dot{M}_* \propto M_g$, increases with M_g, no tight correlation between $L_{\rm nuc,SB}$ and $L_{\rm AGN}$ is seen in LLAGNs. In summary, we suggest that the AGN-starburst connection depends on the evolution of the AGN activity. In order to test our model, it is essential to compare the AGN-starburst luminosity relation for bright AGNs (e.g., Seyfert galaxies and QSOs) with that for LLAGNs.

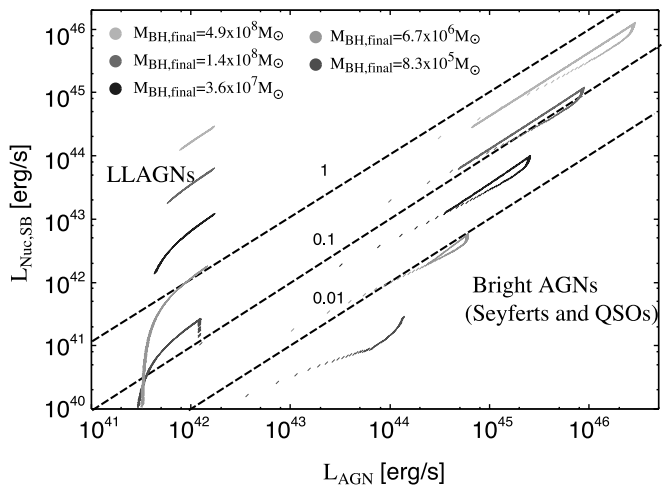

FIG. 8.—Nuclear starburst luminosity, $L_{\rm nuc,SB}$, against the AGN luminosity, $L_{\rm AGN}$. The dots with different colors denote the different final BH mass, $M_{\rm BH,final}$. The dashed lines represent the luminosity ratio, $L_{\rm nuc,SB}/L_{\rm AGN} = 0.01$, 0.1, and 1. [*See the electronic edition of the Journal for a color version of this figure*.]

4. DISCUSSION

4.1. *Effects of AGN Outflow*

Throughout this paper, we assume that all the gas is accreted by a central BH, i.e., $\dot{M}_{\rm BH} = \dot{M}(r_{\rm in})$ even when the mass accretion rate at $r_{\rm in}$ exceeds the Eddington limit (we call this model "model 1"). According to the recent two-dimensional radiation hydrodynamic simulations (e.g., Ohsuga et al. 2005), the super-Eddington mass accretion actually can be achieved, but they mentioned that a large part of the accreting gas turns into outflow because of the strong radiation pressure from the accretion disk (Ohsuga et al. 2005; Ohsuga 2007).

We here assume that the dynamics of the circumnuclear disk is not affected by the outflow. The two models of AGN outflow are possible when $\dot{M}(r_{\rm in}) > \dot{M}_{\rm Edd}$ as follows.

1. The BH grows by a super-Eddington rate, but part of the accreting matter forms outflow, "model 2,"

$$\dot{M}_{\rm outflow} = f_w \dot{M}(r_{\rm in}),$$
$$\dot{M}_{\rm BH} = (1 - f_w)\dot{M}(r_{\rm in}),$$

where we assume $f_w = 0.1$ from the results of Ohsuga (2007).

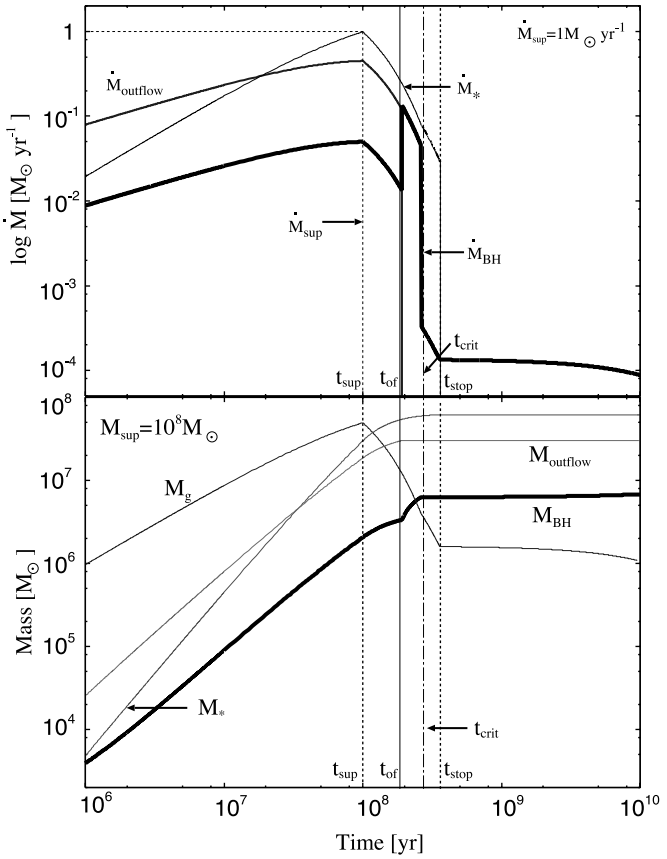

FIG. 9.—Same as Figs. 2 and 3, but the outflow rate ($\dot{M}_{outflow}$) and the total outflow mass ($M_{outflow}$) are newly added for model 2, i.e., super-Eddington growth of SMBHs with the AGN outflow. Here, t_{of} is the time when $\dot{M}(r_{in}) = \epsilon_{BH}^{-1}\dot{M}_{Edd}$. [*See the electronic edition of the Journal for a color version of this figure.*]

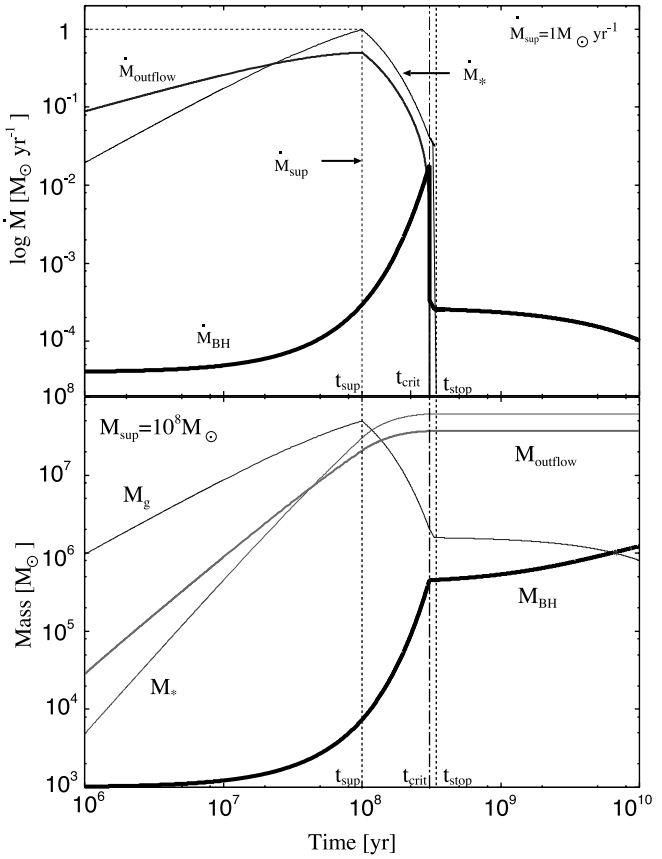

FIG. 10.—Same as Figs. 2 and 3, but the outflow rate ($\dot{M}_{outflow}$) and the total outflow mass ($M_{outflow}$) are newly added for model 3, i.e., Eddington-limited growth of SMBHs with the AGN outflow. [*See the electronic edition of the Journal for a color version of this figure.*]

2. The growth of BHs is regulated by the Eddington limit, and the remnant of accreting gas turns into the outflow, "model 3,"

$$\dot{M}_{outflow} = \dot{M}(r_{in}) - \dot{M}_{BH},$$
$$\dot{M}_{BH} = \epsilon_{BH}^{-1}\dot{M}_{Edd},$$

where $\epsilon_{BH} = 0.05$ is the energy conversion efficiency.

Figure 9 is the same as Figures 2 and 3, but the outflow rate ($\dot{M}_{outflow}$) and the total outflow mass ($M_{outflow}$) are considered based on model 2, where $M_{outflow} \equiv \int_0^t \dot{M}_{outflow}(t')dt'$. During $t < t_{of}$, where t_{of} is the time when $\dot{M}(r_{in}) = \epsilon_{BH}^{-1}\dot{M}_{Edd}$, the SMBH grows by the super-Eddington mass accretion rate, but most of the accreting mass from the gas disk is blown away as the AGN outflows. After $t = t_{of}$, all the gas accrete onto a central BH by less than the Eddington limit (i.e., no AGN outflow). After $t = t_{crit}$, the evolutions are the same as the case without the outflow, i.e., model 1. As seen in Figure 9, we find that the final mass of SMBHs is $M_{BH,final} \simeq 8 \times 10^6\ M_\odot$, which is a factor 4 smaller compared with the prediction by model 1. In model 1, the super-Eddington accretion mainly determines the final SMBH mass (see Figs. 2 and 3). But, in model 2 the contribution of super-Eddington accretion is comparable to that of Eddington accretion to the final SMBH mass. This indicates that the contribution of super-Eddington accretion depends on the strength of AGN outflows, i.e., f_w. Therefore, it will be worth revealing which physics controls f_w by using the radiation hydrodynamic simulations.

On the other hand, we show the case of Eddington-limited BH growth (i.e., model 3) in Figure 10. Apparently, the BH growth is greatly suppressed by AGN outflow, and consequently, the final SMBH is an order of magnitude less than model 1, namely, $M_{BH,final} \simeq 10^6\ M_\odot$. In summary, we find that the evolution of SMBHs is closely linked with not only the state of the circumnuclear disk, but also the strength of the AGN outflow and the conditions under which the super-Eddington growth occurs.

4.2. *Effects on the UV Radiation Pressure*

So far, we have ignored the effect of radiation pressure, but the UV radiation from young stars in the gas disks may affect the vertical structure of disk. Thus, we examine whether the radiation pressure is really negligible when the disk geometry is determined by the SN feedback. If the disk is optically thick to the UV radiation, the radiation pressure (P_{rad}) is given by

$$P_{rad} = l_{SB}/c \simeq 0.14\epsilon S_*(r)h_{tub}(r)c, \tag{17}$$

where $h_{tub}(r)$ is determined by equation (5). Here, $l_{SB} = 0.14\epsilon S_*(r)h(r)c^2$ is the starburst luminosity per unit area.

As a result, the ratio of the radiation pressure and the turbulent pressure via SN explosions ($P_{tub} = \rho_g v_t^2$) can be obtained as follows,

$$\frac{P_{rad}}{P_{tub}} \sim \eta_{-3}^{-1/2}\left(\frac{t_{dyn}}{t_*}\right)^{1/2}, \tag{18}$$

where $t_{dyn} = (r^3/GM_{BH})^{1/2}$ is the dynamical timescale. Because of $t_{dyn}(r_{out})/t_* \sim 10^{-2}$ for the relatively high star formation efficiency, i.e., $C_* = 10^{-8}\ yr^{-1}$, the radiation pressure is neglected as

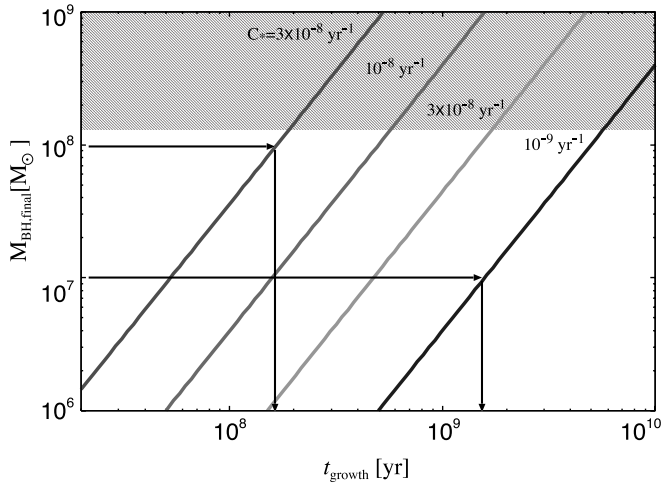

FIG. 11.—Final SMBH mass, $M_{\rm BH,final}$, against the timescale of the SMBH growth without the AGN outflow (model 1). The solid lines with different colors correspond to the different star formation efficiencies. The shaded region denotes the parameter space of $M_{\rm BH,final}$ which is difficult to achieve in the present model. [*See the electronic edition of the Journal for a color version of this figure.*]

far as $\eta > 10^{-5}\ M_\odot^{-1}$. This condition ($\eta > 10^{-5}\ M_\odot^{-1}$) is satisfied for the turbulent pressure-supported starburst disk modeled by WN02 using three-dimensional hydrodynamical simulations. Thus, our conclusions do not change significantly even if we consider the UV radiation pressure.

4.3. *Origin of a Bias in AGN Formation*

Thanks to a growing number of multiwavelength observations at different redshifts, it has been suggested that the density of more luminous AGNs associated to more massive SMBHs peaks earlier in the history of the universe than that of low-luminosity ones (Miyaji et al. 2000; Ueda et al. 2003; Hasinger et al. 2005; Bongiorno et al. 2007). This evolution has been dubbed as AGN cosmic downsizing. It is still unclear why the growth timescale of SMBHs is shorter in more massive SMBHs, in other words, why the growth time is highly biased in an environment to form massive SMBHs. From equation (14), the final SMBH mass can be described as

$$M_{\rm BH,final} \approx 10^8\ M_\odot \left(\frac{C_*}{10^{-8}\ {\rm yr}^{-1}}\right)^2 \left(\frac{t_{\rm growth}}{5\times 10^8\ {\rm yr}}\right)^2. \quad (19)$$

The AGN downsizing might be explained by our result, if larger $M_{\rm BH,final}$ grows in the circumnuclear disk with a higher star formation efficiency. For instance, Figure 11 shows that the growth timescale for $M_{\rm BH,final} = 10^8\ M_\odot$ is shorter than that for $M_{\rm BH,final} = 10^7\ M_\odot$, i.e., $t_{\rm growth}(M_{\rm BH,final} = 10^8\ M_\odot) \approx 10^8$ yr and $t_{\rm growth}(M_{\rm BH,final} = 10^7\ M_\odot) \approx 10^9$ yr, if $C_*(M_{\rm BH,final} = 10^8\ M_\odot)$ is $\approx$30 times as large as $C_*(M_{\rm BH,final} = 10^7\ M_\odot)$. Wada & Norman (2007) showed that the star formation rate increases extensively as a function of the average gas density. Since the massive galaxies could be formed in an environment with a higher average gas density, the star formation efficiency could be $\approx$10 times larger if the average gas density is $\approx$10 times higher. As a consequence, the UV radiation field would be stronger in more massive galaxies. The recent radiation hydrodynamics simulations showed that the critical density for the star formation can be affected by the UV radiation (e.g., Susa & Umemura 2004). These works indicate that the critical density is larger for a stronger UV radiation field. In addition, the star formation efficiency, C_*, would be larger for a larger critical density at a given average gas density (Wada & Norman 2007). Therefore, since the circumnuclear disk in more massive galaxies is exposed to the stronger UV radiation, the star formation efficiency is larger for the gas disk in massive galaxies. Therefore, the strength of the UV radiation field surrounding the galactic nuclei might control the timescale for SMBH growth. In order to clarify this issue, it is essential to examine the star formation process in the gas disk under an intense UV field with the three-dimensional radiation transfer.

5. CONCLUSIONS

We have elucidated the physical role of the circumnuclear disk in relation to SMBH growth. To this end, we have constructed a new model of SMBH growth, taking into account the evolution of physical states of the circumnuclear disk formed by the mass supply from the host galaxy. In the present model, we consider the two regimes of gas accretion depending on the gravitational stability of the disk. Our main conclusions are summarized as follows.

1. Not all the gas in the disk accretes onto the SMBH, i.e., $\dot{M}_{\rm BH} = 0.1$–$0.3\ M_\odot\ {\rm yr}^{-1}$ for $\dot{M}_{\rm sup} = 1\ M_\odot\ {\rm yr}^{-1}$, because part of the gas is used to form stars in the disk. This high-accretion phase changes to the low-accretion phase with $\dot{M}_{\rm BH} \sim 10^{-4}\ M_\odot$ yr. But the transition takes $\sim 10^8$ yr after the mass supply from the host is stopped. This timescale is basically determined by the star formation timescale, $t_* \simeq C_*^{-1} \sim 3\times 10^7$ yr. Through this evolution, the gas-rich disk turns into the gas-poor stellar disk. In the high-accretion phase, a super-Eddington accretion is possible, and thus, the existence of gas-rich circumnuclear disks ($M_g > M_{\rm BH}$) is a condition which the super-Eddington accretion onto a central SMBH keeps. In the present model, the two phases of SMBH growth depend on whether stars can form in the inner region of the circumnuclear disk. This would imply that the AGN activity depends on the spatial distribution of young stars in the circumnuclear disk. In order to examine this, infrared observations with high spatial resolution (e.g., Very Large Telescope Interferometer [VLTI], *Space Infrared Telescope for Cosmology and Astrophysics* [*SPICA*], and the 3 m Atlantic infrared telescope) are crucial, because young stars would be buried in the optically thick circumnuclear disk.

2. Evolution of nuclear activities is divided into four phases: (*i*) the super-Eddington luminosity phase, (*ii*) the sub-Eddington luminosity phase, (*iii*) the starburst luminosity–dominated phases, and (*iv*) the post-AGN phase. Judging from the luminosity ratio, $L_{\rm AGN}/L_{\rm Edd}$, NLS1s or ULIRGs may correspond to phase (*i*). If this is the case, it is predicted that they have gas-rich tori, whose masses are larger than the mass of their central SMBHs. It indicates that the SMBH growth proceeds in the phase surrounded by gas-rich tori. Phase (*ii*) may correspond to BLS1s or QSOs. In this phase, we predict that the gas fraction of the circumnuclear disk is smaller than that for NLS1s or ULIRGs, i.e., $f_g \sim 10\%$–50%. Finally, phases (*iii*) and (*iv*) may correspond to the low-luminosity AGNs (LLAGNs). According to our prediction, LLAGNs have gas-poor (gas fraction $f_g \sim 1\%$) circumnuclear disks. This result suggests that the physical states of circumnuclear gas or stellar systems are important to understanding the nature of different types of AGNs for gas components with ALMA and/or VLTI for stellar components.

3. The final SMBH mass ($M_{\rm BH,final}$) is not proportional to the total gas mass supplied from the host galaxy ($M_{\rm sup}$) during the hierarchical formation of galaxies, i.e., $M_{\rm BH,final}/M_{\rm sup}$ decreases with $M_{\rm sup}$, because the star formation rate overcomes the growth rate of SMBHs as $M_{\rm sup}$ increases. Considering the plausible mass accretion processes from the host galaxy, our results may indicate

that it is difficult to form $\approx 10^9\ M_\odot$ SMBHs observed for high-z QSOs only by the gas accretion process due to the turbulent viscosity via SN explosions. This might imply the importance of alternative mechanisms for the formation of a $\sim 10^9\ M_\odot$ SMBH.

4. The AGN luminosity ($L_{\rm AGN}$) tightly correlates with the nuclear starburst luminosity ($L_{\rm nuc,SB}$) in the bright AGNs (Seyfert galaxies and QSOs). We also predict that $L_{\rm nuc,SB}/L_{\rm AGN}$ is larger for more luminous AGNs (i.e., QSOs). This is not the case in the LLAGNs. Therefore, the preset model predicts that the $L_{\rm AGN}$ versus $L_{\rm nuc,SB}$ relation depends on the evolution of AGN activity.

5. The AGN outflow from the circumnuclear disk greatly suppresses the growth of the SMBHs, especially if the BH growth is limited by the Eddington rate when the mass accretion from the disk exceeds the Eddington limit. This indicates that the strength of AGN outflows affects the evolution of SMBHs and the final mass of SMBHs.

We appreciate the detailed reading and the fruitful comments of anonymous referees. We thank K. Ohsuga, R. I. Davies, and T. Saitoh for useful discussions. K. W. is supported by Grants-in-Aid for Scientific Research (15684003 and 16204012 [K. W.]) of JSPS.

REFERENCES

Abramowicz, M. A., Czerny, B., Lasota, J. P., & Szuszkiewicz, E. 1988, ApJ, 332, 646
Adams, F. C., Graff, D. S., & Richstone, D. O. 2001, ApJ, 551, L31
Antonucci, R. 1993, ARA&A, 31, 473
Balbus, S. A., & Hawley, J. F. 1991, ApJ, 376, 214
Barvainis, R. 1992, ApJ, 400, 502
Bongiorno, A., et al. 2007, A&A, 472, 443
Chiaberge, M., Capetti, A., & Celotti, A. 1999, A&A, 349, 77
Davies, R. I., et al. 2007, ApJ, 671, 1388
Di Matteo, T., Croft, R. A. C., Springel, V., & Hernquist, L. 2003, ApJ, 593, 56
Di Matteo, T., Springel, V., & Hernquist, L. 2005, Nature, 433, 604
Elitzur, M., & Shlosman, I. 2006, ApJ, 648, L101
Fan, X., et al. 2001, AJ, 122, 2833
Granato, G. L., De Zotti, G., Silva, L., Bressan, A., & Danese, L. 2004, ApJ, 600, 580
Hao, C. N., Xia, X. Y., Mao, S., Wu, H., & Deng, Z. G. 2005, ApJ, 625, 78
Hasinger, G., Miyaji, T., & Schmidt, M. 2005, A&A, 441, 417
Heger, A., Fryer, C. L., Woosley, S. E., Langer, N., & Hartmann, D. H. 2003, ApJ, 591, 288
Hönig, S. F., & Becket, T. 2007, MNRAS, 380, 1172
Imanishi, M., & Wada, K. 2004, ApJ, 617, 214
Kawaguchi, T. 2003, ApJ, 593, 69
Kawakatu, N., Andreani, P., Granato, G. L., & Danese, L. 2007a, ApJ, 663, 924
Kawakatu, N., Imanishi, M., & Nagao, T. 2007b, ApJ, 661, 660
Kawakatu, N., & Umemura, M. 2002, MNRAS, 329, 572
Kawakatu, N., Umemura, M., & Mori, M. 2003, ApJ, 583, 85
Kawata, D., & Gibson, B. K. 2005, MNRAS, 358, L16
Kennicutt, R. C., Jr. 1998, ApJ, 498, 541
King, A. 2003, ApJ, 596, L27
Kishimoto, M., et al. 2007, A&A, 476, 713
Kormendy, J., & Richstone, D. 1995, ARA&A, 33, 581
Laor, A., & Draine, B. T. 1993, ApJ, 402, 441
Levine, R., et al. 2008, ApJ, 678, 154
Machida, M., Hayashi, M. R., & Matsumoto, R. 2000, ApJ, 532, L67
Machida, M., & Matsumoto, R. 2003, ApJ, 585, 429
Marconi, A., & Hunt, L. K. 2003, ApJ, 589, L21
Mathur, S., et al. 2000, MNRAS, 314, L17
McLure, R. J., Jarvis, M. J., Targett, T. A., Dunlop, J. S., & Best, P. N. 2006, MNRAS, 368, 1395
Mihos, J. C., & Hernquist, L. 1994, ApJ, 431, L9
———. 1996, ApJ, 464, 641
Miyaji, T., Hasinger, G., & Schmidt, M. 2000, A&A, 353, 25
Ohsuga, K. 2007, ApJ, 659, 205
Ohsuga, K., et al. 2005, ApJ, 628, 368
Okamoto, T., Nemmen, R. S., & Bower, R. G. 2008, MNRAS, 385, 161
Pringle, J. E. 1981, ARA&A, 19, 137
Saitoh, T. R., & Wada, K. 2004, ApJ, 615, L93
Shakura, N. I., & Sunyaev, R. A. 1973, A&A, 24, 337
Silk, J., & Rees, M. J. 1998, A&A, 331, L1
Sitko, M., et al. 1993, ApJ, 409, 139
Suganuma, M., et al. 2006, ApJ, 639, 46
Susa, H., & Umemura, M. 2004, ApJ, 610, L5
Taconni, L., et al. 2006, ApJ, 640, 228
Teng, S. H., Wilson, A. S., Veilleux, S., Young, A. J., Sanders, D. B., & Nagar, N. M. 2005, ApJ, 633, 664
Thompson, T., Quataert, E., & Murray, N. 2005, ApJ, 630, 167 (T05)
Toomre, A., & Toomre, J. 1972, ApJ, 178, 623
Ueda, Y., Akiyama, M., Ohta, K., & Miyaji, T. 2003, ApJ, 598, 886
Umemura, M. 2001, ApJ, 560, L29
Umemura, M., Fukue, J., & Mineshige, S. 1997, ApJ, 479, L97
Urry, C. M., & Padovani, P. 1995, PASP, 107, 803
Wada, K., & Norman, C. A. 2002, ApJ, 566, L21 (WN02)
———. 2007, ApJ, 660, 276
Wada, K., & Tomisaka, K. 2005, ApJ, 619, 93
Watabe, Y., Kawakatu, N., & Imanishi, M. 2008, ApJ, 677, 895
Watarai, K.-Y., Fukue, J., Takeuchi, M., & Mineshige, S. 2000, PASJ, 52, 133
Yamada, M., Wada, K., & Tomisaka, K. 2007, ApJ, 671, 73